



HAL
open science

Jovian High-Latitude Ionospheric Ions: Juno In Situ Observations

P. Valek, F. Allegrini, F. Bagenal, S. Bolton, J. Connerney, R. Ebert, T. Kim, S. Levin, P. Louarn, D. McComas, et al.

► **To cite this version:**

P. Valek, F. Allegrini, F. Bagenal, S. Bolton, J. Connerney, et al.. Jovian High-Latitude Ionospheric Ions: Juno In Situ Observations. *Geophysical Research Letters*, 2019, 46 (15), pp.8663-8670. 10.1029/2019GL084146 . hal-02367844

HAL Id: hal-02367844

<https://hal.science/hal-02367844>

Submitted on 29 Nov 2021

HAL is a multi-disciplinary open access archive for the deposit and dissemination of scientific research documents, whether they are published or not. The documents may come from teaching and research institutions in France or abroad, or from public or private research centers.

L'archive ouverte pluridisciplinaire **HAL**, est destinée au dépôt et à la diffusion de documents scientifiques de niveau recherche, publiés ou non, émanant des établissements d'enseignement et de recherche français ou étrangers, des laboratoires publics ou privés.

Copyright

Geophysical Research Letters

RESEARCH LETTER

10.1029/2019GL084146

Key Points:

- The high-latitude ionosphere is observed between the magnetic latitudes bounded by the auroral oval and Io's magnetic flux shell
- Two populations are observed at high latitudes: (1) magnetospheric ions consisting of H, S, and O ions and (2) cold ionospheric H⁺ ions
- Observation of a loss cone suggests precipitating magnetospheric ions heat the upper ionosphere to heights ~0.5 R_J above the clouds

Correspondence to:

P. W. Valek,
pvalek@swri.edu

Citation:

Valek, P. W., Allegrini, F., Bagenal, F., Bolton, S. J., Connerney, J. E. P., Ebert, R. W., et al. (2019). Jovian high-latitude ionospheric ions: Juno in situ observations. *Geophysical Research Letters*, 46, 8663–8670. <https://doi.org/10.1029/2019GL084146>










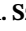



Received 17 JUN 2019

Accepted 26 JUL 2019

Accepted article online 1 AUG 2019

Published online 14 AUG 2019

Jovian High-Latitude Ionospheric Ions: Juno In Situ Observations

P. W. Valek¹ , F. Allegrini^{1,2} , F. Bagenal³ , S. J. Bolton¹ , J. E. P. Connerney^{4,5} , R. W. Ebert^{1,2} , T. K. Kim^{2,1} , S. M. Levin⁶ , P. Louarn⁷ , D. J. McComas⁸ , J. R. Szalay⁸ , M. F. Thomsen⁹ , and R. J. Wilson³ 

¹Southwest Research Institute, San Antonio, TX, USA, ²Department of Physics and Astronomy, University of Texas at San Antonio, San Antonio, TX, USA, ³Laboratory for Atmospheric and Space Physics, University of Colorado Boulder, Boulder, CO, USA, ⁴Space Research Corporation, Annapolis, MD, USA, ⁵Goddard Space Flight Center, Greenbelt, MD, USA, ⁶Jet Propulsion Laboratory, Pasadena, CA, USA, ⁷Université de Toulouse, IRAP, CNRS, UPS, Toulouse, France, ⁸Department of Astrophysical Sciences, Princeton University, Princeton, NJ, USA, ⁹Planetary Sciences Institute, Tucson, AZ, USA

Abstract The low-altitude, high-velocity trajectory of the Juno spacecraft enables the Jovian Auroral Distributions Experiment to make the first in situ observations of the high-latitude ionospheric plasma. Ions are observed to energies below 1 eV. The high-latitude ionospheric ions are observed simultaneously with a loss cone in the magnetospheric ions, suggesting precipitating magnetospheric ions contribute to the heating of the upper ionosphere, raising the scale height, and pushing ionospheric ions to altitudes of 0.5 R_J above the planet where they are observed by Jovian Auroral Distributions Experiment. The source of the magnetospheric ions is tied to the Io torus and plasma sheet, indicated by the cutoff seen in both the magnetospheric and ionospheric plasma at the Io M-shells. Equatorward of the Io M-shell boundary, the ionospheric ions are not observed, indicating a drop in the scale height of the ionospheric ions at those latitudes.

Plain Language Summary The Jovian Auroral Distributions Experiment (JADE) ion sensor has made the first in situ observations of the upper, high-latitude ionosphere of Jupiter. Flown on the Juno spacecraft, JADE observes the ionosphere at altitudes of approximately half a Jovian radii, with the spacecraft traveling at the high speed of ~50 km/s. For comparison, a proton traveling at 50 km/s has an energy of approximately 10 eV. The combination of the low-altitude and high ram velocity enables JADE to measure ionospheric ions to energies below 1 eV. These observations reveal a cold ionospheric population of protons at high latitudes, seen coincident with precipitating magnetospheric ions. This indicates that the precipitating magnetospheric ions heat the upper ionosphere, raising the height where these protons can be observed. The ionospheric protons are seen in bands in the northern and southern latitudes, bounded on the equator edge by the field lines that connect to Io, and inside the auroral oval to the poleward side.

1. Introduction

To date, the exploration of Jupiter's ionosphere has been limited to emissions (ultraviolet and infrared) from ~1,000 km above the cloud deck and from radio occultations by mostly equatorial passes of spacecraft (see review by Yelle & Miller, 2004). The occultation profiles show electron density peaking between 800 and 2,000 km and suggest that temperatures reach ~1200 K (Hinson et al., 1997, 1998). These radio occultation profiles of electron density are each often very noisy, have order of magnitude variations between passes, and are limited to less than 4,000 km about the 1-bar level. Voyager Plasma Science data showed that protons comprise ~10% of the torus and plasma sheet density (Bagenal, 1985; Bodisch et al., 2017). These equatorial protons seemed to be pretty much in thermal equilibrium with the magnetospheric (Iogenic) sulfur and oxygen ions and are thought to come from some combination of solar wind and ionospheric sources (Bagenal & Delamere, 2011). The outflow of ionospheric plasma was proposed (pre-Galileo mission) by Nagy et al. (1986) and estimated to be 2×10^{28} ions per second, which is comparable in number density to the Io source but, assuming that the composition is mostly protons, the mass source rate would be only 35 kg/s. The expected Iogenic mass source rate is ~500 kg/s. Before Juno arrived at Jupiter, there were no direct measurements of ionospheric material between the ionosphere and the plasma sheet.

The Juno mission (Bolton et al., 2017) flies in a polar orbit around Jupiter. Its orbit permits new observations of the Jovian magnetosphere-ionosphere system in previously unexplored magnetospheric regions (Bagenal et al., 2017), including the first, repeated direct observations of the upper, high-latitude ionosphere. We present here the first in situ measurements of the high-latitude ionosphere ion population.

2. Data

The Juno spacecraft (Bolton et al., 2017) is in an elliptical polar orbit around Jupiter with a low perijove (altitude $\sim 3,000$ km). This minimizes the exposure to the intense radiation belts by flying below them during perijove. At higher (approximately subauroral) latitudes the spacecraft is at altitudes of ~ 0.5 R_J ($\sim 35,000$ km). The Juno orbit results in a high spacecraft velocity at perijove of about 60 km/s. For reference, the kinetic energy of a proton traveling at ~ 50 km/s is 10 eV. The low perijove altitude and high ram velocity enable the first, and repeated, direct sampling of the low energy, the upper Jovian ionosphere.

The low-energy plasma population is measured by the Jovian Auroral Distributions Experiment (JADE; McComas et al., 2017). JADE is a suite of electrostatic analyzers that measure the ion and electron plasma population. The ion sensor (JADE-I) measures the ion energy spectrum between 10 eV and 46 keV/q in the spacecraft frame every 2 s. The high spacecraft velocity near perijove permits the observation of ions with energies below 1 eV when the sensor is looking into the ram direction.

The JADE-I sensor has 12 anodes that cover a 270° field of view. The sensor is mounted such that its plane spans across the spacecraft deck, up through the spin axis (i.e., approximately sunward), and then around to point antiparallel to the spin axis. The 180° wide fan between the spin and antispin directions sweeps out the full sky every spacecraft spin (~ 30 -s period).

In addition to measuring the incident ion energy per charge, JADE-I uses a time of flight (TOF) section to measure the mass per charge in the range of 1 to >64 amu/q. After the energy per charge is measured by the electrostatic analyzer, ions are accelerated with a 10-kV potential toward the TOF. The TOF system uses ultrathin carbon foil (Allegrini et al., 2016) for a source of secondary, start electrons. The detection time interval between the start electrons and the primary particle is then used to determine the particle velocity. The mass resolution of the TOF section for low-energy ions is sufficient to separate the light and heavy ions, and O⁺ from S⁺ ($\Delta M/M > 5$). Using higher-order effects related to particle-carbon foil interactions, higher mass resolution can be obtained. A complete discussion of the TOF system, including the higher-order carbon foil effects, is given in Kim et al. (2019).

3. Observations

Juno's trajectory for Perijove 1 (PJ1) is shown in Figure 1a, as viewed from the Sun. The spacecraft travels from north to south near dusk local time. The spacecraft spin axis points out of the plane of panel (a). The periods when the high-latitude ionosphere is observed are indicated by the thick segments on the trajectory line. The ionosphere is also observed at the equator; however, the equatorial observations are not discussed here and will be the topic of a future paper. To help orientate the viewer, a sketch of a magnetic field line is included.

Energy spectrograms showing only protons at high northern and southern latitudes are shown in Figures 1b and 1c (along spin axis) and Figures 1d and 1e (in Juno's spin plane), respectively. For each spectrogram, a background of penetrating particles has been removed by subtracting a baseline of counts seen across all energy steps. As discussed above, the spacecraft velocity is significant when compared to the plasma velocity. The spectrograms are shifted in energy to account for the spacecraft velocity. The gray band at the bottom of each panel indicates the measurement limit. For the anodes that view along the spin axis (i.e., perpendicular to the ram direction, Figures 1b and 1c) this is a small correction and only the upper energy of the ionospheric ions are observed. The correction is significant in the spin plane (Figures 1d and 1e), and ions to below 1 eV are observable in the ram direction. The proton flux observations extend to below 1 eV at times when the spacecraft has rotated such that JADE-I is viewing into the ram direction.

Poleward of the auroral oval (not shown), no low-energy ions are observed. At 1210 UT magnetospheric plasma in the JADE-I energy range are seen. The magnetospheric ions are the population with energies of

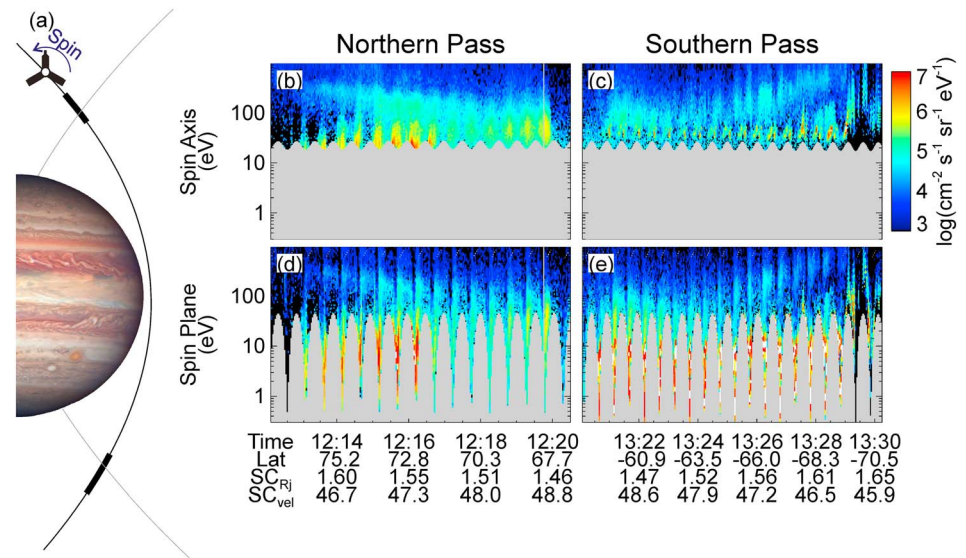


Figure 1. Proton observations during the first Juno peri-jove (PJ1) on 27 August 2016. The path of the spacecraft is shown as viewed from the Sun in panel (a). The spacecraft spin axis is out of the plane. The energy-time spectrograms are shifted in energy to account for the high spacecraft ram velocity. The periods of the observations in the spectrograms are indicated by the thick lines. Observations of protons approximately parallel to the spin axis ($\sim 90^\circ$ pitch angle) are shown in panel (b) for the northern pass (southern pass in panel [c]). The observations approximately in the spin plane are in panels (d) and (e). The spin plane is approximately parallel to both the spacecraft ram direction and local magnetic field directions during the observations shown.

a few hundreds of electron volts that go to lower energies with time (lower latitudes). This population includes both light and heavy ions (heavy ions not shown here), and the velocity distribution is consistent with a corotating population with approximately pickup thermal speeds (see Szalay et al., 2017, for a discussion of this population). Heavier ions (not shown) have a similar energy spectrum as the magnetospheric protons but shifted in energy as they are comoving. The periodic minima seen in the magnetospheric population when viewed in the spin plane (Figures 1d and 1e) are observations of a loss cone. This feature is discussed in more detail below.

Later (equatorward) at ~ 1213 UT, ionospheric ions are observed. The ionospheric ions have lower energy (<100 eV/q) and therefore are not comoving with the magnetospheric population. The ionospheric distribution observed in the ram direction has energies of a few electron volts. Ionospheric ions are most distinct when viewing the ram direction (Figures 1d and 1e), but the upper-energy tail is seen in the spin direction (Figures 1b and 1c).

At 1220, Juno moves equatorward of a boundary where the magnetospheric and ionospheric ions are no longer seen. As the spacecraft travels through the southern hemisphere, a similar pattern is seen (Figures 1c and 1e): Magnetospheric and ionospheric ions are seen at the equatorward boundary, with ionospheric ions with a few electron volts of energy and magnetospheric ions with increasing energy with higher latitude, and at the poleward extent primarily the magnetospheric ions are observed.

The energy-TOF spectrum for a two-spin sample of the northern (southern) pass is shown in Figure 2a (Figure 2b). The TOF data product is collapsed over the look direction to reduce the telemetry size. Solid lines have been added to Figure 2 to indicate the location of common ions. The dashed line indicates the separation between the ionospheric and magnetospheric ions.

The magnetospheric ion population shown in Figure 2 consists of both heavy and light ions comoving with velocities ~ 150 km/s. During the periods shown in this figure the spacecraft is on M-shells of ~ 11 and 12.5 during 1214–1215 and 1327–1328, respectively. M-shell is defined as the radial distance of the magnetic field at the point where it crosses the equator. This is similar to the concept of the L-shell at Earth, but since L-shell was developed for a purely dipolar field, we use the nomenclature of M-shell to distinguish the highly nondipolar plus current sheet field of Jupiter.

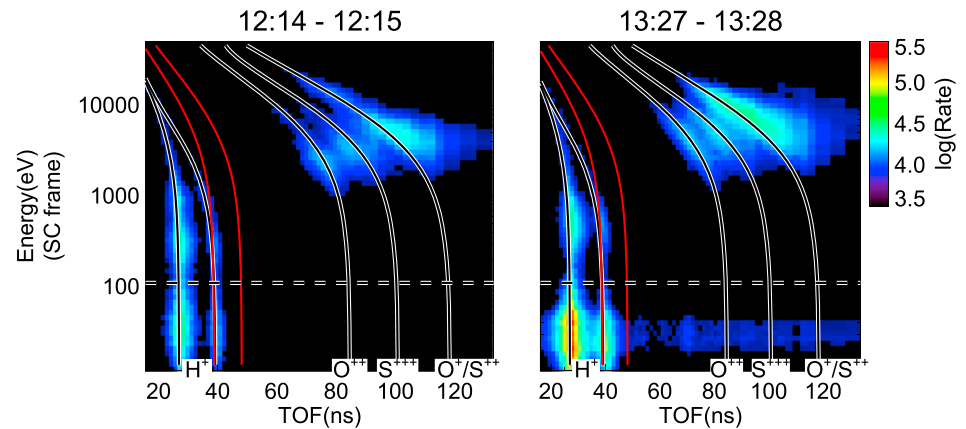


Figure 2. Energy-TOF spectrum of the ionospheric and magnetospheric ions. Solid lines indicate the nominal location for masses of H^+ , O^{++} , S^{+++} , and O^+/S^{+++} (i.e., mass per charge of 1, 8, 10.67, and 16). The red lines are at the locations where H_2^+ and H_3^+ would be observed. Note that the H^+ line is bifurcated with one branch overlapping the H_2^+ line at low energies. The dashed horizontal line indicates the transition energy between the ionospheric and magnetospheric ions. Counts seen at low, ionospheric energies at long TOF are contamination from the proton signal. TOF = time of flight.

The ionospheric protons are observed at energies of a few tens of electron volts in the spacecraft frame and are primarily protons. A dashed line at 100 eV is drawn at the approximate boundary between the ionospheric and magnetospheric populations. This consistently is the energy that ionospheric ions are below in the instrument frame. Most of the time the magnetospheric ions have an energy above 100 eV, however, near the Io boundary, the magnetospheric protons will have a low-energy tail that extends below 100 eV.

The two peaks in the proton TOF signal (~ 40 ns at low energies) is due to the hydrogen exiting the TOF carbon foil with a distribution of charges of approximately 80% H^0 and 20% H^+ (Gonin et al., 1994). Since the TOF section is not field free, the H^+ is slowed and has a longer travel time. This carbon foil effect has been discussed fully and used to separate O^+ and S^{++} ions by Kim et al. (2019). The counts at longer times of flight at low energies (particularly clear in the plot on the right) are from contamination from the proton signal.

The red lines indicate where H_2^+ and H_3^+ are expected to be seen. The H_3^+ ions are not observable at this level. The ratios of the primary to secondary proton peak amplitudes agree with the 80/20 ratio expected for pure protons passing through the TOF. We estimate that there is less than 10% H_2^+ compared to the H^+ in these observations.

For PJ1, the local magnetic field (Connerney et al., 2017) direction was observed to be approximately in the spin plane for the periods highlighted in Figure 1. When JADE-I views along the antiparallel (parallel) direction of the field line in the northern (southern) hemisphere a loss cone of the distribution is observed. The loss cone is indicated by a dropout in counts from the magnetospheric population (Figures 1b and 1d). These dropouts are not observed when viewing a $\sim 90^\circ$ pitch angle (Figures 1c and 1e).

To highlight the loss cone, spectrograms for a limited time range are shown in Figures 3a and 3c. The arrows above the spectrogram in panel a (c) indicate the times when JADE-I is viewing antiparallel (parallel) to the magnetic field line or times when outflowing ions would be seen. Reductions in the ion flux of outward flowing magnetospheric ions are clear.

The lower panels in Figures 3b and 3d are plots of the velocity distributions for the periods indicated by the vertical bars in the panels above. The gray circle near the center denotes the low-energy cutoff of the sensor and is shifted off center due to the large ram speed. The magnetospheric protons are seen at higher velocities of a few hundreds of kilometers per second. When JADE-I is more poleward (i.e., larger magnetic shells), the observed magnetospheric ions have higher velocities.

In the velocity distribution plots, there is a clear loss cone. To guide the eye, we have drawn in lines representing a 28° loss cone. This loss cone was estimated using a loss cone angle of $\sim \sin^{-1}(1/R^3)^{1/2}$ assuming that the magnetic field strength goes as $1/R^3$. This loss cone is consistent with the observed precipitating electron

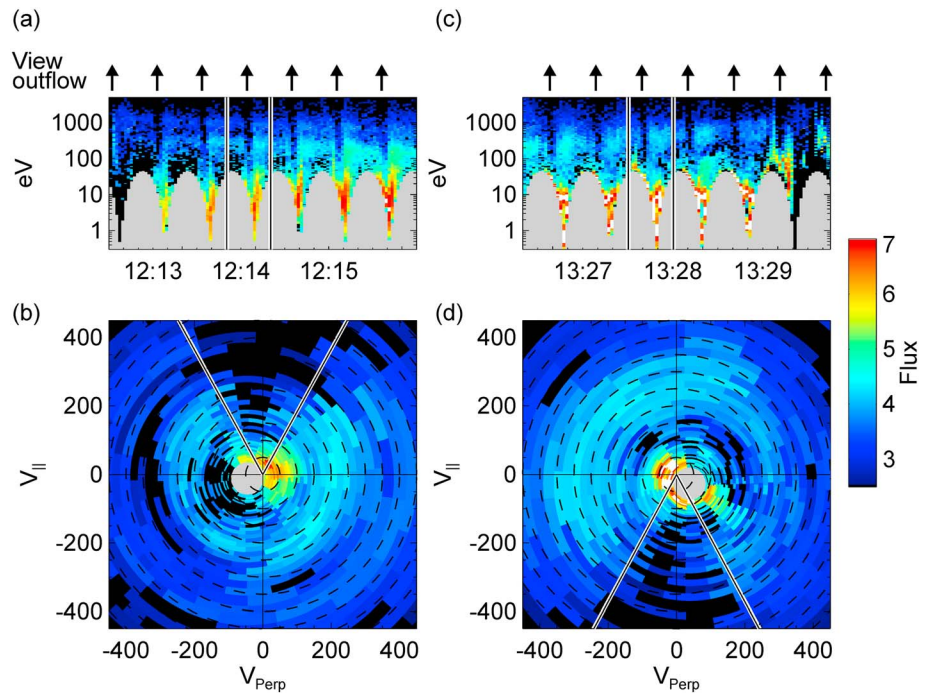


Figure 3. Energy-time spectrograms for a section of the northern (a) and southern (c) passes shown in Figure 1. The arrows indicate times when outflowing ions would be viewed. Below (b and d) are plots of the velocity distributions for the time range indicated by the vertical lines. The dashed circles are spaced every 50 km/s, and the gray color indicates the lower limit of the measurement. The angled lines in (b) and (d) are at $\pm 28^\circ$ from the outflowing direction. The spectrograms and velocity distributions are plotted in the Jupiter frame.

loss cone observed by the Juno/JEDI instrument (Mauk et al., 2017). The 30-s spin rate coupled with the 2-s energy sweep rate results in angular measurements with an $\sim 24^\circ$ resolution for JADE-I.

The ionospheric ions are seen near the center with velocities below ~ 100 km/s. The full distribution is not observable, but the distribution appears to be more extended in the v_{perp} direction than the v_{parallel} direction.

When observations from multiple perijoves are collected together, a pattern emerges of where the ionospheric ions are located. Figure 4 shows low-energy protons (<150 eV in the spacecraft frame) plotted as a function of latitude and longitude (panels a and c) for Perijoves 1 through 16. Note that the plots have uniform spacing of degrees latitude rather than an orthographic projection of the planet's poles. The energy range was chosen to focus on the ionospheric component. However, near the Io magnetic flux shell boundary, the magnetospheric plasma does extend to low energies and some magnetospheric flux may be included in this plot (cf. Figure 1).

In Figure 4 the magnetic foot point of Io's orbit and the nominal auroral ovals are drawn in as solid black lines. The foot paths of the magnetic flux shell threading Io's orbit (Io M-shell) are determined using the JRM09 internal magnetic field model (Connerney et al., 2018) plus a simple equatorial current sheet (Connerney et al., 1981). The inner and outer auroral boundaries are from observations by Hubble Space Telescope (Bonfond et al., 2012, 2017).

Figure 4 shows how the ionospheric flux is concentrated between the Io M-shell and auroral oval. The flux has a more pronounced boundary at the Io M-shell boundary than at the auroral oval. This band where the ionospheric flux is enhanced is at the same latitudes where the loss cone is observed in the magnetospheric plasma (Figure 3).

Poleward of the auroral oval the low ion energy flux is typically not observable by JADE. A slightly enhanced flux is seen equatorward of the Io M-shell for some of the northern passes, and most of the southern passes. This is due to a background from penetrating particles when Juno is passing through the radiation belts. It is

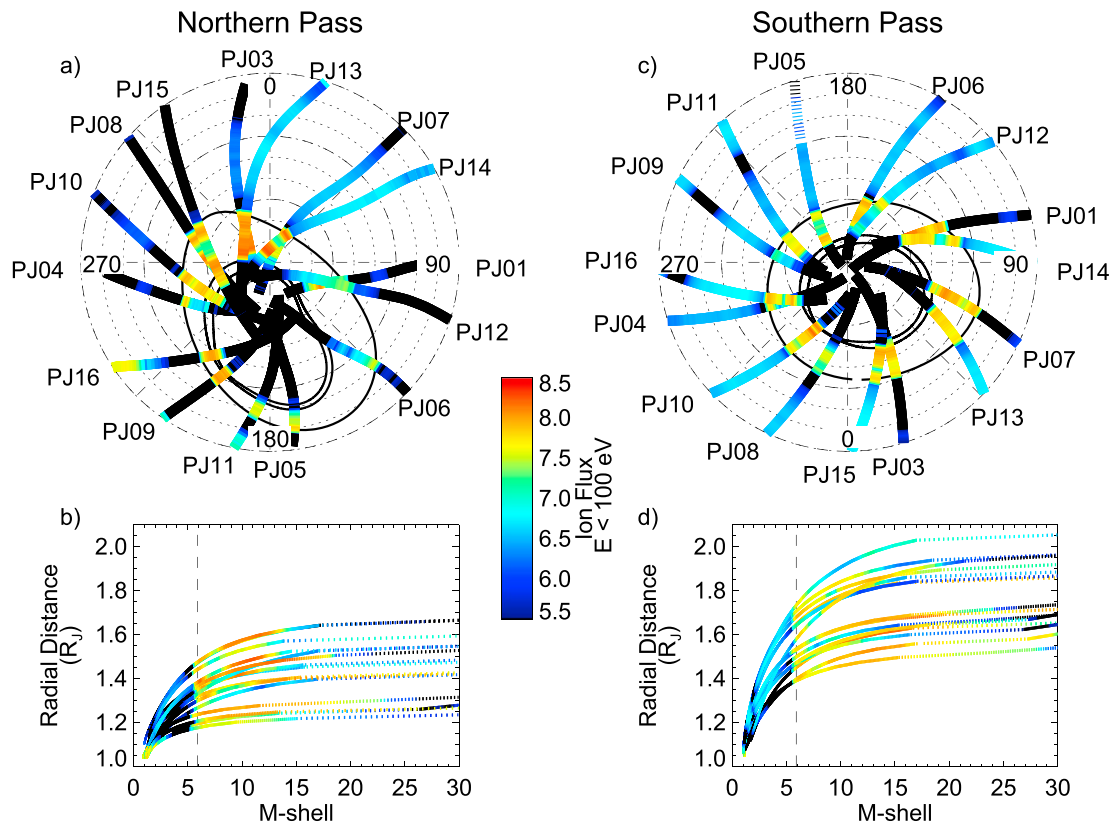


Figure 4. Ion flux from PJ1 through PJ16. Panels (a) and (c) show the flux as a function of the latitude and longitude of the magnetic foot point for the northern and southern passes. The latitude circles are 5° apart. The foot points of the Io orbit and the auroral oval are drawn in as solid black lines. Below, the same flux values are plotted as a function of the spacecraft radial distance versus M-shell. The vertical dashed line is at an M-shell of 5.9 (i.e., Io orbit).

more pronounced in the southern hemisphere due to the higher altitudes of these orbits, (i.e., Juno typically flies below the radiation belts in the northern hemisphere).

The same flux values are plotted as a function of the spacecraft radial distance and the magnetic shell (M-shell) in Figures 4b and 4d. This mapping is only performed for M-shells less than 30, the approximate location of the auroral oval (Connerney et al., 2018).

In Figures 4b and 4d, Io's M-shell is indicated with the dashed line at $M = 5.9$. Note again the sharp increase in ionospheric flux poleward (higher M-shells) of the Io foot point boundary. Above M-shell of ~ 15 , the ion flux drops, indicating changes in the magnetosphere at those distances. This is seen in Figures 4b and 4d where the flux drops by approximately an order of magnitude going to larger M-shells, though the flux is generally still higher than equatorward of the Io boundary. Inside the Io foot point, the background from the radiation belts is more pronounced at higher altitudes, or Jovicentric distances greater than $\sim 1.3 R_J$.

4. Discussion and Conclusions

The low-altitude, high-velocity trajectory of the Juno spacecraft enables JADE-I to make the first in situ observations of the high-latitude ionospheric plasma. JADE-I's ability to measure low-energy ions, coupled with high spacecraft velocity, extends the observations to energies below 1 eV when viewing in the ram direction.

Since the high-latitude ionospheric ions are observed simultaneously with a loss cone in the magnetospheric ions, we suggest that the precipitating magnetospheric ions contribute to the heating of the upper ionosphere, raising the scale height, and pushing ionospheric ions to altitudes of $0.5 R_J$ above the planet where they are observed by JADE. The source of the magnetospheric ions is tied to the Io torus and plasma sheet,

indicated by the cut off seen in both the magnetospheric and ionospheric plasma at the Io M-shells. Equatorward of the Io M-shell boundary, the ionospheric ions are not observed, indicating a drop in the scale height of the ionospheric ions at those latitudes.

We summarize the results as follows:

1. JADE-I does not observe low-energy, ionospheric ions poleward of the auroral oval.
2. Between the auroral oval and the Io foot point, magnetospheric ions are seen. The magnetospheric ions are identified by their composition consisting of light (H^+) and heavy (O^{n+} , S^{n+}) ions and having a velocity consistent with corotation.
3. The magnetospheric ions also have a loss cone, suggesting recent precipitation. The loss cone width is consistent with a magnetic field that varies as $1/R^3$.
4. Equatorward of the auroral oval, ionospheric ions are seen. These ions consist primarily of protons and have energies of a few electron volts observed in the ram direction.
5. The ionospheric ions are consistently seen between M-shells of 5.9 (i.e., the Io foot point) and 10–15. The high-latitude ionospheric ions are only observed coincident with precipitating (lost cone distribution) magnetospheric ions.

In this paper we present a preliminary analysis of ions observed close to Jupiter at high latitudes. Clearly, such flux tubes connect to the plasma sheet in the equatorial middle magnetosphere. In future work we aim to make a more quantitative analysis of these Juno-JADE-I data, deriving plasma parameters such as flow speed, density, temperature, and anisotropy, as well as composition. Such parameters and their extrapolation along the field line will be key for understanding the magnetosphere-ionosphere coupling of the Jovian magnetosphere.

Calculation of the moments is challenging due to the gap in the lowest-energy observations (see Figure 3). However, a numerical integration of the protons with energies below 100 eV gives densities on the order of tens of per cubic centimeter for the high-latitude, topside ionosphere. Future moments calculations will include modeling of the distribution to fill in the low-energy part of the distribution that is in the antiram direction. However, if we use a density of 30 cm^{-3} and an outflow 10^{28} s^{-1} , we can estimate of an outflow speed of $\sim 20 \text{ km/s}$. This indicates that the predicted outflow rate of Nagy et al. (1986) is reasonable, and the ionosphere may be a significant source of Jovian magnetospheric plasma.

Acknowledgments

This work was supported as a part of the work on NASA's Juno mission. We thank the many individuals who continue to make the Juno mission such a success. The JNO-I/SW-JAD-3-CALIBRATED-V1.0 and JNO-SS-3-FGM-CALIBRATED-V1.0 data sets were obtained from the Planetary Data System (PDS; <https://pds.nasa.gov/>).

References

- Allegrini, F., Ebert, R. W., & Funsten, H. O. (2016). Carbon foils for space plasma instrumentation. *Journal of Geophysical Research: Space Physics*, *121*, 3931–3950. <https://doi.org/10.1002/2016JA022570>
- Bagenal, F. (1985). Plasma conditions inside Io's orbit: Voyager measurements. *Journal of Geophysical Research*, *90*(A1), 311–324. <https://doi.org/10.1029/JA090iA01p00311>
- Bagenal, F., Adriani, A., Allegrini, F., Bolton, S. J., Bonfond, B., Bunce, E. J., et al. (2017). Magnetospheric science objectives of the Juno mission. *Space Science Reviews*, *213*(1-4), 219–287. <https://doi.org/10.1007/s11214-014-0036-8>
- Bagenal, F., & Delamere, P. A. (2011). Flow of mass and energy in the magnetospheres of Jupiter and Saturn. *Journal of Geophysical Research*, *116*, A05209. <https://doi.org/10.1029/2010JA016294>
- Bodisch, K. M., Dougherty, L. P., & Bagenal, F. (2017). Survey of Voyager plasma science ions at Jupiter: 3. Protons and minor ions. *Journal of Geophysical Research: Space Physics*, *122*, 8277–8294. <https://doi.org/10.1002/2017JA024148>
- Bolton, S. J., Lunine, J., Stevenson, D., Connerney, J. E. P., Levin, S., Owen, T. C., et al. (2017). The Juno mission. *Space Science Reviews*, *213*(1-4), 5–37. <https://doi.org/10.1007/s11214-017-0429-6>
- Bonfond, B., Grodent, D., Gérard, J.-C., Stallard, T., Clarke, J. T., Yoneda, M., et al. (2012). Auroral evidence of Io's control over the magnetosphere of Jupiter. *Geophysical Research Letters*, *39*, L01105. <https://doi.org/10.1029/2011gl050253>
- Bonfond, B., Saur, J., Grodent, D., Badman, S. V., Bisikalo, D., Shematovich, V., et al. (2017). The tails of the satellite auroral footprints at Jupiter. *Journal of Geophysical Research: Space Physics*, *122*, 7985–7996. <https://doi.org/10.1002/2017ja024370>
- Connerney, J. E. P., Acuña, M. H., & Ness, N. F. (1981). Modeling the Jovian current sheet and inner magnetosphere. *Journal of Geophysical Research*, *86*(A10), 8370–8384. <https://doi.org/10.1029/JA086iA10p08370>
- Connerney, J. E. P., Benn, M., Bjarno, J. B., Denver, T., Espley, J., Jorgensen, J. L., et al. (2017). The Juno magnetic field investigation. *Space Science Reviews*, *213*(1-4), 39–138. <https://doi.org/10.1007/s11214-017-0334-z>
- Connerney, J. E. P., Kotsiaros, S., Oliverson, R. J., Espley, J. R., Joergensen, J. L., Joergensen, P. S., et al. (2018). A new model of Jupiter's magnetic field from Juno's first nine orbits. *Geophysical Research Letters*, *45*, 2590–2596. <https://doi.org/10.1002/2018GL077312>
- Gonin, M., Kallenbach, R., & Bochsler, P. (1994). Charge exchange of hydrogen atoms in carbon foils at 0.4–120 keV. *Review of Scientific Instruments*, *65*(3), 648–652. <https://doi.org/10.1063/1.1145132>
- Hinson, D. P., Flasar, F. M., Kliore, A. J., Schinder, P. J., Twicken, J. D., & Herrera, R. G. (1997). Jupiter's ionosphere: Results from the first Galileo radio occultation experiment. *Geophysical Research Letters*, *24*(17), 2107–2110. <https://doi.org/10.1029/97GL01608>
- Hinson, D. P., Twicken, J. D., & Karayel, E. T. (1998). Jupiter's ionosphere: New results from Voyager 2 radio occultation measurements. *Journal of Geophysical Research*, *103*(A5), 9505–9520. <https://doi.org/10.1029/97JA03689>

- Kim, T. K., Ebert, R. W., Valek, P. W., Allegrini, F., McComas, D. J., Bagenal, F., et al. (2019). Method to Derive Ion Properties from Juno JADE Including Abundance Estimates for O⁺ and S²⁺. *Journal of Geophysical Research: Space Physics*. <https://doi.org/10.1029/2018ja026169>
- Mauk, B. H., Haggerty, D. K., Paranicas, C., Clark, G., Kollmann, P., Rymer, A. M., et al. (2017). Juno observations of energetic charged particles over Jupiter's polar regions: Analysis of monodirectional and bidirectional electron beams. *Geophysical Research Letters*, *44*, 4410–4418. <https://doi.org/10.1002/2016GL072286>
- McComas, D. J., Alexander, N., Allegrini, F., Bagenal, F., Beebe, C., Clark, G., et al. (2017). The Jovian Auroral Distributions Experiment (JADE) on the Juno mission to Jupiter. *Space Science Reviews*, *213*(1–4), 547–643. <https://doi.org/10.1007/s11214-013-9990-9>
- Nagy, A. F., Barakat, A. R., & Schunk, R. W. (1986). Is Jupiter's ionosphere a significant plasma source for its magnetosphere? *Journal of Geophysical Research*, *91*(A1), 351–354. <https://doi.org/10.1029/JA091iA01p00351>
- Szalay, J. R., Allegrini, F., Bagenal, F., Bolton, S., Clark, G., Connerney, J. E. P., et al. (2017). Plasma measurements in the Jovian polar region with Juno/JADE. *Geophysical Research Letters*, *44*, 7122–7130. <https://doi.org/10.1002/2017gl072837>
- Yelle, R. V., & Miller, S. (2004). Jupiter: The planet, satellites, and magnetosphere, chap. 9. In *Jupiter's thermosphere and ionosphere*. Cambridge: Cambridge University Press.